Enthalpy relaxation of low molecular weight PMMA: a strategy to evaluate the Tool–Narayanaswamy–Moynihan model parameters

2003 J. Phys.: Condens. Matter 15 S1215

(http://iopscience.iop.org/0953-8984/15/11/339)

INSTITUTE OF PHYSICS PUBLISHING JOURNAL OF PHYSICS: CONDENSED MATTER

J. Phys.: Condens. Matter **15** (2003) S1215–S1226 PII: S0953-8984(03)58329-1

Enthalpy relaxation of low molecular weight PMMA: a strategy to evaluate the Tool–Narayanaswamy–Moynihan model parameters

L Andreozzi, M Faetti, M Giordano and D Palazzuoli

Dipartimento di Fisica, Università di Pisa, via F Buonarroti 2 Pisa I-56127, Italy
and
INFM, UdR Pisa, Italy

Received 20 October 2002
Published 10 March 2003
Online at stacks.iop.org/JPhysCM/15/S1215

Abstract

The enthalpy recovery mechanism of a low molecular weight synthesis of polymethylmethacrylate is investigated by means of differential scanning calorimetry (DSC) experiments. The experimental results can be described satisfactorily in terms of the Tool–Narayanaswamy–Moynihan theory. This work is mainly focused on developing a strategy for evaluation of the best set of parameters for the model. The approach starts with a simultaneous fitting procedure of several experimental DSC traces. Sets of parameters are obtained which exhibit agreement with experiments. The enthalpy lost on ageing of the sample in the glassy state as a function of the annealing time is then compared with the predictions provided by using the different sets of parameters. We show that this procedure is able to single out the best set of parameters and to provide a good estimation of the Adam–Gibbs temperature.

1. Introduction

The main peculiarity of the glassy state is its out-of-equilibrium thermodynamic character. If a glass is kept in isothermal conditions below its glass transition temperature, its physical properties spontaneously change as the material attempts to achieve an equilibrium state [1, 2]. This slow dynamic process is usually referred to as structural relaxation or physical ageing, and characterizes different classes of materials such as low molecular weight inorganic glass formers, polymers, spin glasses, dipolar glasses and so on. Phenomenological and molecular approaches to the structural relaxation of glasses have been proposed in the past [3–6]. At variance with the relaxation behaviour in the supercooled region, in physical ageing one has to consider the nonlinear character of the process. In the phenomenological model of Tool, Narayanaswamy and Moynihan (the TNM model), this is ensured by a dependence of the instantaneous relaxation times on both the temperature and the structure of the system that changes during ageing. As a structural parameter, a fictive temperature T_f is usually introduced

which indeed represents an attempt to associate the equilibrium state at $T = T_f$ to the out-of-equilibrium state at the actual temperature T. This approach, intensively tested in dilatometric and calorimetric experiments, is able to describe the structural relaxation mechanism fairly well, even if some problems have been evidenced, especially in polymeric systems [2]. In particular, the model introduces fit parameters, which should be material parameters. However, some differential scanning calorimetry (DSC) experiments reported in the literature showed that the best fit parameters depended on the thermal history of the samples [7–9]. It should be noted that these effects cannot be fully accounted for by experimental errors (mainly thermal lag) which broaden the overshooting peaks in the DSC thermograms recorded after the ageing. Therefore some modifications of the TNM model have been proposed [10, 11]. An additional question regards the determination of the best fit parameters. These are usually obtained by simultaneously fitting several experimental thermograms (an alternative procedure is found in [12]). However, due to the strong correlation among the parameters [2, 13], one of them has to be kept fixed during the fit. In this way several different sets of model parameters are obtained and there is a need for a discriminating criterion. In this paper we present a DSC experimental study of the enthalpy relaxation of a low molecular weight PMMA sample and propose a procedure for the evaluation of the best TNM parameters.

2. Theoretical section

The TNM model has been well described in several review articles [2] so that we give here only the main assumptions and constitutive equations. The non-exponential character of structural relaxation is considered by assuming as a relaxation function the stretched exponential

$$\Phi(t) = \exp\left[-\left(\frac{t}{\tau}\right)^{\beta}\right] \tag{1}$$

with τ as the relaxation time and β the shape parameter. The latter is considered constant by invoking the time–temperature superposition principle [2]. In order to take into account nonlinearity a fictive temperature T_f is introduced as a structural parameter [14]. T_f is defined by the relation

$$H(T) = H_{eq}(T_f) - \int_T^{T_f} C_p^{glass}(\theta)\,\mathrm{d}\theta \tag{2}$$

where $H_{eq}(T_f)$ is the equilibrium value of the enthalpy H at temperature T_f and $C_p^{glass}(T)$ is the unrelaxed glassy heat capacity. The instantaneous relaxation time τ is assumed to depend on both the actual temperature and the fictive temperature which changes during the ageing process. The problem is then linearized by defining a reduced time

$$\xi(t) = \int_0^t \frac{\mathrm{d}t'}{\tau(t')}$$

and using the Boltzmann superposition principle [2]. Accordingly one obtains an explicit expression for the evolution of the fictive temperature after a selected thermal treatment:

$$T_f(T) = T_0 + \int_{T_0}^{T} \mathrm{d}T' \left\{1 - \exp\left(-\left[\int_{T'}^{T} \frac{\mathrm{d}T''}{Q\tau(T_f, T'')}\right]^{\beta}\right)\right\} \tag{3}$$

where T_0 is a reference temperature well above the glass transition temperature and $Q = Q_{c,h}$ is the cooling/heating rate. If an annealing procedure is employed at a temperature T_a for a time t_a, the term

$$\int_0^{t_a} \frac{\mathrm{d}t'}{\tau(T_f(t'), T_a)}$$

must be added to the reduced time calculus in the second integration. By numerical integration of equation (3), the normalized heat capacity $C_p^N \equiv \mathrm{d}T_f/\mathrm{d}T$ can be evaluated and compared with the corresponding experimental quantity obtained by differentiating equation (2):

$$\frac{\mathrm{d}T_f}{\mathrm{d}T} = \frac{(C_p(T) - C_p^{glass}(T))}{\Delta C_p(T_f)} \approx \frac{(C_p(T) - C_p^{glass}(T))}{\Delta C_p(T)} \equiv C_p^N(T) \tag{4}$$

where $\Delta C_p(T) = C_p^{liq} - C_p^{glass}$ is the heat capacity increment between the glassy and liquid states. The model is completed by choosing a proper expression for the instantaneous relaxation times $\tau(T, T_f)$. The most widely used are the generalized Arrhenius expression proposed by Narayanaswamy [3] and Moynihan (NM) [4]:

$$\tau(T_f, T) = A \exp\left\{\frac{x\,\Delta h}{RT} + \frac{(1-x)\Delta h}{RT_f}\right\} \tag{5}$$

and the one proposed by Scherer and Hodge (SH) [13]:

$$\tau(T_f, T) = A \exp\left\{\frac{B}{RT(1 - T_2/T_f)}\right\}. \tag{6}$$

Hodge showed [15] that, for experiments not too far from equilibrium, these expressions are quite similar as far as the predictive power of the model is concerned. However, some differences may be appreciated for experiments at quite low temperatures and for very different annealing times [7, 16] as the SH relation provides better agreement with the experimental curves. Furthermore it resolves some of the controversial aspects of the NM expression, such as the Arrhenius behaviour for equilibrium relaxation times and unphysical values obtained for the pre-exponential factor A [2]. Finally, the SH expression can be derived by extending the Adam–Gibbs (AG) theory to the out-of-equilibrium case, while the NM one is empirical in character. Even though it was derived several years ago [17], the AG theory and the related Kauzmann problem is still widely discussed in the literature [18]. In this framework, modelling structural relaxation in nonlinear enthalpy relaxation experiments could represent an alternative way to obtain the AG temperature T_2 (see equation (6)). However, the best parameters cannot trivially be found from DSC experiments. In fact, as already remarked, because of the strong correlation in the parameters of equation (6), the fits of the DSC traces are carried out for several fixed values of the AG temperature (or the pseudo-activation energy B). Consequently one usually obtains sets of parameters which provide similar agreement between theory and experiments. In order to single out the most appropriate value of the AG temperature one should avail oneself of some additional information. A procedure in current use is based on the relation between the value of the activation energy Δh at the glass transition and the cooling rate dependence of the glass transition temperature [2, 4]:

$$\frac{\Delta h}{R} = -\left.\frac{\mathrm{d}\ln Q_c}{\mathrm{d}(1/T_g)}\right|_{T_g}. \tag{7}$$

In equation (7) the glass transition temperature T_g is defined as the glassy value of the fictive temperature, obtained by the intersection of the liquid enthalpy curve with the asymptotic glassy enthalpy curve. From this, one can fix a value for the parameter Δh in the fit of the experimental DSC traces adopting the expression of equation (5). Then with some approximate relations among the parameters of equations (5) and (6) [15] the AG temperature can be found. This procedure, however, presents several shortcomings. Firstly equation (7) has been recently criticized and a more general scaling law has been proposed [19]. Then the relations between x and Δh in equation (5), and B and T_2 in equation (6), are approximate in character, being that the two expressions are not fully equivalent. Finally, due to the limited realizable range

Table 1. Best fit parameters found by the search routine in the simultaneous fitting procedure for different AG temperature settings.

T_2 (K)	B (kJ mol^{-1})	A (s)	β	$T_g - T_2$ (K)
207	59 880	7.2×10^{-27}	0.47	110
217	50 014	1.7×10^{-24}	0.45	100
237	35 121	3.4×10^{-21}	0.41	80
249	25 387	8.8×10^{-18}	0.39	68
257	20 277	6.7×10^{-16}	0.38	60

of cooling rates, the value of Δh obtained from equation (7) usually has a large uncertainty, of the order of 20%. Consequently the AG temperature can be collocated only in a broad temperature range [20]. Thus it seems that an alternative way to determine the best choice for the AG temperature in modelling enthalpy relaxation experiments should be found.

3. Experimental procedure

The PMMA sample was purchased from Labservice Analytica Anzola Emilia (BO), Italy and used as received. The weight average molecular weight was $M_w = 1460$ g mol^{-1}, corresponding to about 10 monomeric units. The polydispersity was $M_w/M_N = 1.07$. The glass transition temperature, obtained by using the enthalpic definition [21] for a cooling rate of 40 K min^{-1}, was $T_g = 317.3$ K.

DSC measurements were carried out with a Perkin-Elmer DSC 7 frequently calibrated with indium and zinc standards. Highly pure nitrogen was used as a purge gas. The experimental protocol is reported here: the sample was maintained at the temperature $T = T_g + 50$ for some minutes in order to erase any previous treatment, then it was cooled at a fixed rate Q_c to the selected starting temperature ($T_g - 80$) of the scan. Finally it was heated at 10 K min^{-1} on recording the signal. For most of the experiments, the cooling rate was fixed at $Q_c = 40$ K min^{-1}, and an annealing procedure at the chosen temperature T_a for a selected annealing time t_a was carried out before cooling to $T_g - 80$. After each experiment, a reference scan (cooling/heating with rates 40 and 10 K min^{-1}, respectively) was immediately recorded to evaluate the enthalpy lost due to the ageing.

4. Results and discussion

In a recent paper [22] we have shown that the TNM model with equation (6) describes fairly well the enthalpy relaxation in this low molecular weight PMMA. In particular, the model parameters from fitting single DSC scans were not greatly affected by the thermal history dependence and it was possible to simultaneously fit several different DSC traces with good agreement with respect to every single experimental thermogram. We carried out simultaneous fitting procedures, by means of the Nedler–Mead search routine [23], for several T_2 settings in the range 187 K $< T_2 <$ 277 K. In figure 1, the best fits obtained for $T_2 = 237$ K are superimposed on the experiments. The value $T_2 = 237$ K provided the lowest total square deviation, but comparable agreement was found for different choices. In table 1 some of the different sets of best fit parameters are reported. The same parameters are also able to satisfactorily reproduce the simpler cooling/heating scans, as showed in figure 2 ($T_2 = 237$ K). The fitting procedure aims to reproduce the position and shape of the overshooting peaks appearing in the DSC traces. These are strongly dependent on the annealing conditions, but their shape is also affected by experimental errors so that it is difficult to select a single set of

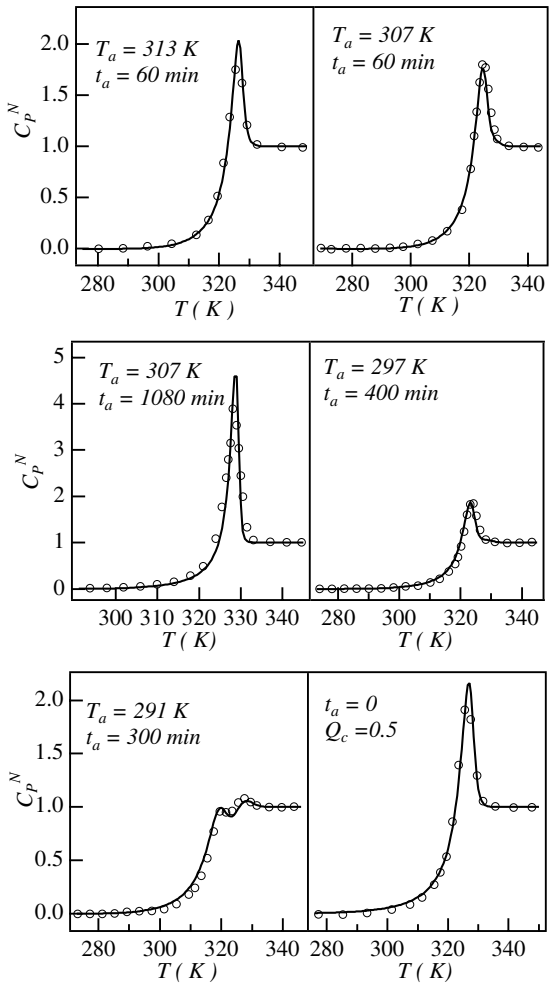

Figure 1. Best fits obtained with a simultaneous fit of six different DSC traces. The thermal histories are reported in the figures. Model parameters are from table 1 at ($T_2 = 237$ K).

parameters via simultaneous fitting. From the point of view of the structural dynamics of the system it must be noted that the shape of the overshooting peaks is related to the behaviour of the out-of-equilibrium instantaneous relaxation times during the heating scan. These in turn are mainly determined by the same parameters A, B, T_2 defining the equilibrium temperature dependence of the relaxation times of equation (6). Furthermore the different set of parameters of table 1 provide very similar $\log \tau$ versus $1000/T$ plots in a narrow range of temperature around the glass transition, as showed in figure 3. The finding is consistent with the good agreement of the calculated and experimental traces for the different sets of parameters.

A deeper insight into the problem of singling out a best fit set is provided by the observation that not only the shape and the position of the DSC peaks are relevant, but also the area enclosed under the peaks has a physical meaning. In fact, it is easily related to the value of the enthalpy lost during the annealing step in the glassy state [2, 9] $\Delta H(T_a, t_a)$:

$$\Delta H(T_a, t_a) = \int_{T_x}^{T_y} (C_p^a(\theta) - C_p^u(\theta))\, \mathrm{d}\theta \tag{8}$$

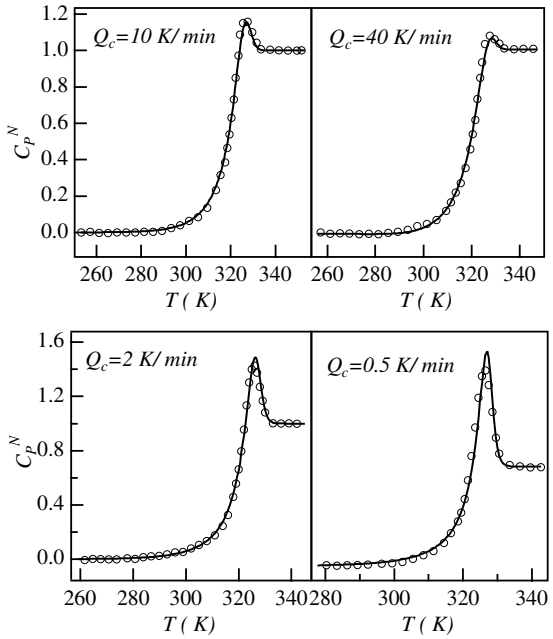

Figure 2. Simple cooling/heating DSC experiments (markers) and theoretical predictions of the TNM model obtained with the parameters reported in table 1 for ($T_2 = 237$ K). Cooling rates are reported in the figures.

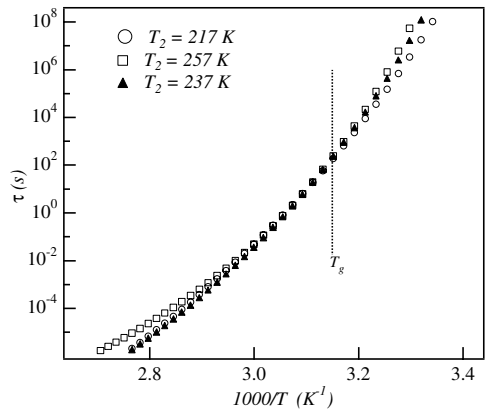

Figure 3. Temperature dependence of the equilibrium relaxation times (see equation (6)) calculated for some of the different sets of parameters of table 1.

where $C_p^a(T)$ and $C_p^u(T)$ are the heat capacity measured after annealing the sample at T_a for the time t_a, and the heat capacity of the unannealed sample, respectively. T_x and T_y are reference temperatures where the two signals overlap ($T_x < T_g < T_y$). This procedure actually provides the experimental enthalpy difference after the two thermal treatments (with and without the annealing) at the starting scan temperature ($T_g - 80$ K in this study). It represents only an approximation by defect of the enthalpy lost during the annealing step, which becomes very reliable only for low enough annealing temperatures [7, 22]. However, it has a clear physical

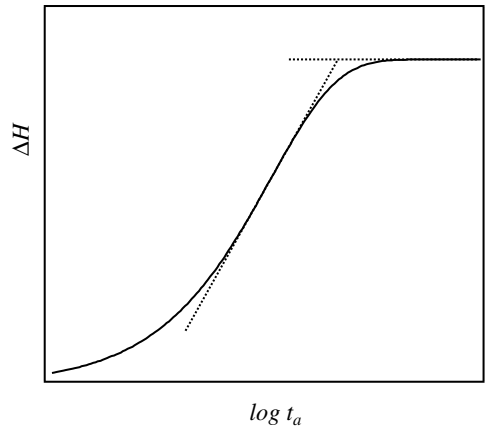

Figure 4. Typical schematic behaviour of the enthalpy lost on ageing a glass as a function of the annealing time. Inflectional slope defining the relaxation rate R_H, and plateau value of ΔH are depicted in the figure.

meaning and is largely unaffected by experimental errors such as thermal lag or baseline shifts. If the smooth temperature dependence of the configurational heat capacity near T_g is neglected, $\Delta C_p = C_p^{liq} - C_p^{glass} \approx \Delta C_p(T_g)$, the values experimentally obtained with equation (8) have to be compared with the quantity obtained with the model:

$$\Delta H(T_a, t_a) = \Delta C_p(T_g)\{T_f^u(T_g - 80) - T_f^a(T_g - 80)\} \tag{9}$$

where the value of $T_f^u(T_g - 80)$ represents the model prediction of the glass transition temperature. This procedure allows one to single out the best set of model parameters, which in such a way turn out to have been tested against a large amount of experimental data.

In figure 4, an idealized behaviour of $\Delta H(T_a, t_a)$ as a function of $\log t_a$ is shown. The enthalpy relaxation process is characterized by the key features, relaxation rate and plateau value shown in the plot. The relaxation rate $R_H(T_a)$ is defined as the inflectional slope of the relaxation isotherm:

$$R_H(T_a) = \left.\frac{\mathrm{d}\Delta H(T_a, t_a)}{\mathrm{d}\log t_a}\right|_{inf}. \tag{10}$$

This parameter, first introduced by Kovacs [24], turns out to be useful in comparing the relaxation kinetics of different glass forming systems. Recently an approximate expression for the relaxation rate has been proposed [25] in terms of the TNM parameters. The second important feature is represented by the plateau value, which depends on the limit glassy state attained at long times. In the framework of the TNM model this is mainly determined by the difference $T_g - T_a$. It can be observed that, while the simultaneous fit aims to reproduce the shape and position of the DSC peaks, the study of the enthalpy relaxation isotherms leads to considering the tails of the $C_P(T)$ curves and the values predicted for the glass transition temperature.

In figure 5 the experimental results concerning $\Delta H(T_a, t_a)$ at three different annealing temperatures are presented. A broad time range is clearly seen where $\Delta H(T_a, t_a)$ shows a linear dependence on $\log t_a$, from which the relaxation rates $R_H(T_a)$ are evaluated according to equation (10). In figure 6 the experimental $R_H(T_a)$ are compared with the prediction of the TNM model for some different AG temperatures (complete sets of parameters in table 1). The best agreement between theory and experiments is found for $T_2 = 237$ K $\approx T_g - 80$ K;

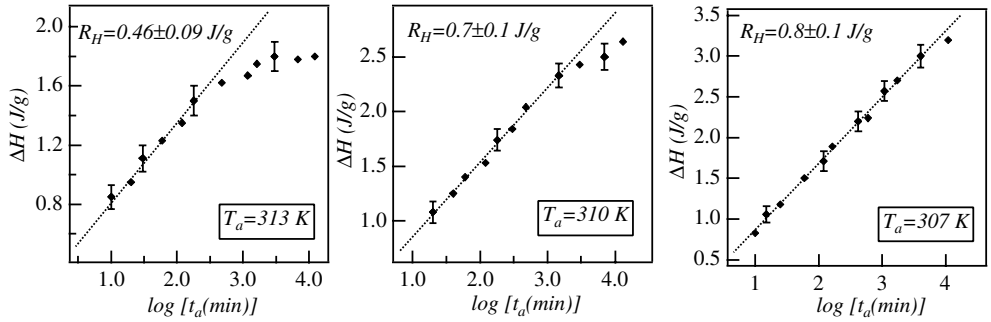

Figure 5. Experimental enthalpy relaxation isotherms at three different annealing temperatures. The experimental values of the relaxation rate are reported in the figures.

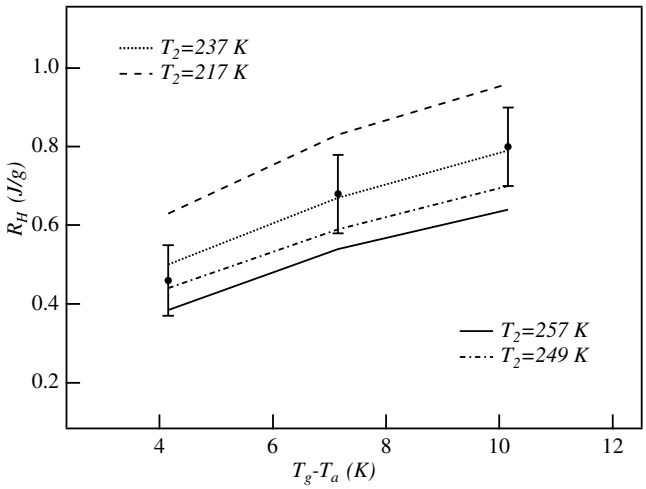

Figure 6. Comparison between the experimental relaxation rates, and the theoretical predictions from the TNM model for different sets of parameters (AG temperatures are given in the figure; the other parameters are in table 1).

Table 2. Asymptotic glassy value of fictive temperature after cooling at 40 K min^{-1}, as predicted by the TNM model for the different sets of parameters of table 1.

T_2 (K)	207	217	237	249	257
T_g (K)	318.5	318.1	317.3	316.3	315.9

the results obtained for $T_2 = 217$ and 257 K are outside the experimental errors whereas the setting $T_2 = 249$ K marks the highest limit for the AG temperature.

In order to complete the analysis of the relaxation isotherms, the values of $\Delta H(T_a, t_a)$ as a function of log t_a must be directly compared. In fact, besides the relaxation rate, the prediction of the glass transition temperature, or equivalently the integral fit of the reference scan, plays an important role. In table 2 the values of the glassy fictive temperature after cooling at 40 K min^{-1} are reported for some sets of parameters. Interestingly the better agreement with the experimental value is found for the set identified by $T_2 = 237$ K. Furthermore, a rapid inspection of table 2 shows the systematic dependence of the theoretical prediction of

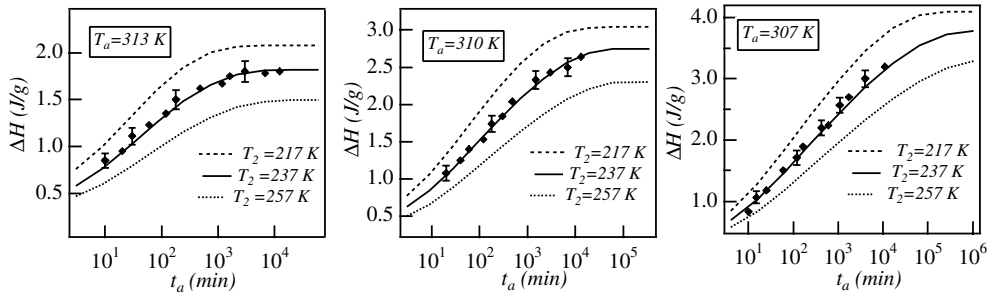

Figure 7. Experimental $\Delta H(T_a, t_a)$ as a function of the annealing times, and corresponding model predictions for some of the different sets of parameters found by the search routine (table 1). The annealing temperatures are indicated in the figures.

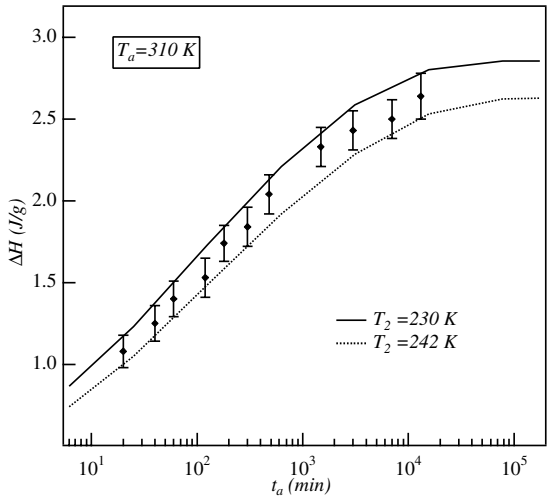

Figure 8. Experimental $\Delta H(T_a, t_a)$ values obtained with ageing experiments at $T = 310$ K (dots). The curves are theoretical predictions of the TNM model for two sets of parameters found by the search routine after simultaneous fitting of the six DSC scans shown in figure 1. Parameters: dotted curve $A = 6 \times 10^{-20}$ s, $B = 31\,134$ kJ mol^{-1}, $\beta = 0.4$; full curve: $A = 1.1 \times 10^{-22}$ s, $B = 40\,570$ kJ mol^{-1}, $\beta = 0.42$.

the glass transition temperature on the AG temperature setting. This leads one to think that the quantitative comparison between the experimental $\Delta H(T_a, t_a)$ data and the corresponding theoretical predictions (equation (9)) could represent a severe test to discriminate between the different sets of parameters. In figure 7 such comparisons are shown for experiments at the three annealing temperatures. The theoretical predictions pertaining to the setting $T_2 = 237$ K always provide a good description of the experimental data, whereas the others show a clear disagreement. In this analysis, we estimated the uncertainty in the T_2 value performing additional simultaneous fits to evaluate $\Delta H(T_a, t_a)$. In figure 8 the results of this analysis are shown for the annealing experiments carried out at $T_a = 310$ K. These results suggest locating the AG temperature in the range 230 K $< T_2 <$ 242 K. Similar conclusions were drawn considering additional annealing temperatures. These limits are probably too restrictive because they do not take into account the approximations employed in the evaluation of $\Delta H(T_a, t_a)$ and the experimental errors in $\Delta C_P(T_g)$ itself. Nevertheless the above study

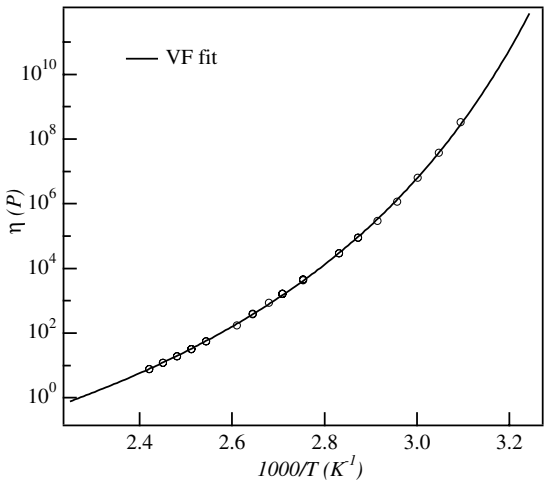

Figure 9. Temperature dependence of the shear viscosity in this low molecular weight PMMA sample. The line is the best fit obtained with the Vogel–Fulcher law.

strongly supports the results obtained from analysis of the relaxation rates R_H, which are largely independent of errors in $\Delta C_P(T_g)$. This allows one to set $T_2 = 237 \pm 10$ K. T_2 being the temperature where the equilibrium relaxation times diverge, it plays a central role in AG theory from which the SH expression (equation (6)) is derived. Indeed a crucial test for the AG theory is the comparison between the AG temperature and the Vogel temperature T_0. The latter is the divergence temperature in the Vogel–Fulcher law that usually describes the relaxation experiments fairly well [26, 27]:

$$\tau(T) = A \exp\left[\frac{B}{R(T - T_0)}\right]. \tag{11}$$

We performed viscoelastic measurements in this PMMA sample, in the linear response regime, by means of a rheometer (Haake Rheostress RS 150), which applied a controlled shear stress to the sample. Due to the range of frequencies ($10^{-2} < \omega < 10^{-4}$) covered by our measurements, the master curve was reconstructed via the time–temperature superposition principle. The temperature dependence of the shift factor a_T was then used to give the viscosity curve. Reference values of viscosity were obtained with experiments in the time domain for the highest temperatures. In figure 9 the temperature dependence of the shear viscosity η is shown and the line in the figure is the best fit obtained assuming equation (11). The Vogel temperature was found to be $T_0 = 249 \pm 8$ K, in good agreement with the AG temperature obtained by modelling the nonlinear enthalpy relaxation experiments. The pseudo-activation energy B was found to be $B = 20.3 \pm 0.5$ kJ mol^{-1}, appreciably lower than the corresponding value drawn from the simultaneous fitting of the DSC curves (see table 1). This implies that the two relaxation plots provide different values for the steepness index m, which is a measure of the kinetic fragility [28]:

$$m = \left.\frac{\mathrm{d}\log\tau}{\mathrm{d}(T_g/T)}\right|_{T_g}. \tag{12}$$

It is worth noting that the enthalpy recovery experiments give $m \approx 91$ for $T_2 = 237$ K, which agrees with the value $m = 96$ given by the cooling rate dependence of the glass transition temperature (see equation (7)). In contrast, the temperature dependence of viscosity leads to

the quite lower value $m = 72$. This finding could be related to an inappropriate use of the time–temperature superposition principle. In fact, in several unentangled low molecular weight polymers, the local segmental relaxation time showed a temperature dependence stronger than viscosity [27]. However the observed discrepancy could also be partially related to the different temperature range of enthalpy relaxation measurements and viscoelastic analysis. In this respect, a recent paper [29] has shown that the AG equation is able to describe the relaxation process in different glass forming systems only in a reduced temperature range $T_g < T < T_B$. T_B was found to be qualitatively coincident with the critical temperature found by Stickel and co-workers [30] where a dynamics change is observed in several systems. These topics could be profitably investigated, comparing results found from the enthalpy relaxation measurements and the ones from experimental techniques probing the segmental dynamics.

5. Conclusions

In this work we presented a study carried out by means of DSC experiments on the enthalpy relaxation mechanism in a low molecular PMMA. We showed that the TNM model, with the Scherer–Hodge expression for the instantaneous relaxation times, was able to simultaneously reproduce several different thermograms. However, due to the experimental errors and the strong correlation between the model parameters, the simultaneous fitting procedure was unable to select a single set of model parameters. The major objective of this work was to propose an experimental procedure for the best evaluation of the model parameters with particular respect to the AG temperature. To this aim, we compared theoretical predictions and experimental results pertaining to three isothermal enthalpy relaxation curves. Such curves are less rich in information than the complex specific shape of the DSC thermograms. On the other hand, they are largely independent of the experimental errors affecting DSC scans. Such a procedure allowed us to single out the best set of model parameters ($T_2 = 237$ K) and to reduce to about 20 K the spread in the AG temperature determination. The value of the AG temperature was then compared with the Vogel temperature obtained by viscoelastic measurements. The temperatures were found to be coincident within the experimental errors, but the shear viscosity showed a temperature dependence smoother than the enthalpic relaxation times.

References

[1] Struick L C E 1978 *Physical Aging in Amorphous Polymers and Other Materials* (Houston: Elsevier Science)
[2] Hodge I M 1994 *J. Non-Cryst. Solids* **169** 211
[3] Narayanaswamy O S 1971 *J. Am. Ceram. Soc.* **54** 491
[4] Moynihan C T, Easteal A J, DeBolt M A and Tucker J 1976 *J. Am. Ceram. Soc.* **59** 12
[5] Kovacs A J, Aklonis J J, Hutchinson J M and Ramos A R 1979 *J. Polym. Sci. Polym. Phys. Ed.* **17** 1097
[6] Drozdov A D 1999 *Phys. Lett.* A **258** 158
[7] Gómez Ribelles J L, Ribes Greus A and Diaz Calleja R 1990 *Polymer* **31** 223
[8] Tribone J J, O'Really J M and Greener J 1986 *Macromolecules* **19** 1732
[9] Cowie J M G and Ferguson R 1993 *Polymer* **34** 2135
[10] Gómez Ribelles J L and Monleón Pradas M 1995 *Macromolecules* **28** 5867
[11] Hutchinson J M, Montserrat S, Calventus Y and Cortés P 2000 *Macromolecules* **33** 5252
[12] Hutchinson J M and Ruddy M J 1988 *J. Polym. Sci. Polym. Phys. Ed.* **26** 2341
[13] Hodge I M 1987 *Macromolecules* **20** 2897
Scherer G W 1984 *J. Am. Ceram. Soc.* **67** 504
[14] Tool A Q 1946 *J. Am. Ceram. Soc.* **29** 240
[15] Hodge I M 1997 *J. Res. Natl Inst. Stand. Technol.* **102** 195
[16] Andreozzi L, Faetti M, Giordano M and Palazzuoli D 2002 *Phil. Mag.* B **82** 397
[17] Adam G and Gibbs J H 1965 *J. Chem. Phys.* **43** 139

[18] Dixon P K 1990 *Phys. Rev.* B **42** 8179
Casalini R, Capaccioli S, Lucchesi M, Rolla P A and Corezzi S 2001 *Phys. Rev.* E **64** 031207
Johari G P 2000 *J. Chem. Phys.* **113** 751
Johari G P 2001 *J. Non-Cryst. Solids* **288** 148
[19] Mascarell J B and Belmonte G G 2000 *J. Chem. Phys.* **113** 4965
[20] Hodge I M and O'Really J M 1999 *J. Phys. Chem.* B **103** 4171
[21] Richardson M J and Savill N G 1975 *Polymer* **16** 753
[22] Andreozzi L, Faetti M, Giordano M and Palazzuoli D 2002 submitted
[23] Nedler J A and Mead R 1965 *Comput. J.* **7** 308
[24] Kovacs A J 1958 *J. Polym. Sci.* **30** 131
[25] Malek J 1998 *Macromolecules* **31** 8312
[26] Rault J 2000 *J. Non-Cryst. Solids* **271** 177
[27] Ngai K L 2000 *J. Non-Cryst. Solids* **275** 7
[28] Böhmer R and Angell C A 1992 *Phys. Rev.* B **45** 10091
[29] Richert R and Angell C A 1998 *J. Chem. Phys.* **108** 9016
[30] Stickel F, Fischer E W and Richert R 1995 *J. Chem. Phys.* **102** 6251